

The sensitivity enhancement of TiO₂-based VOCs sensor decorated by gold at room temperature

Shooshtari, Mostafa; Vollebregt, Sten; Vaseghi, Yas; Rajati, Mahshid; Pahlavan, Saeideh

DOI

[10.1088/1361-6528/acc6d7](https://doi.org/10.1088/1361-6528/acc6d7)

Publication date

2023

Document Version

Final published version

Published in

Nanotechnology

Citation (APA)

Shooshtari, M., Vollebregt, S., Vaseghi, Y., Rajati, M., & Pahlavan, S. (2023). The sensitivity enhancement of TiO₂-based VOCs sensor decorated by gold at room temperature. *Nanotechnology*, 34(25), Article 255504. <https://doi.org/10.1088/1361-6528/acc6d7>

Important note

To cite this publication, please use the final published version (if applicable). Please check the document version above.

Copyright

Other than for strictly personal use, it is not permitted to download, forward or distribute the text or part of it, without the consent of the author(s) and/or copyright holder(s), unless the work is under an open content license such as Creative Commons.

Takedown policy

Please contact us and provide details if you believe this document breaches copyrights. We will remove access to the work immediately and investigate your claim.

PAPER • OPEN ACCESS

The sensitivity enhancement of TiO₂-based VOCs sensor decorated by gold at room temperature

To cite this article: Mostafa Shooshtari *et al* 2023 *Nanotechnology* **34** 255501

View the [article online](#) for updates and enhancements.

You may also like

- [Improved Gas Sensing Performance of ALD AZO 3-D Coated ZnO Nanorods](#)
P. Lin, X. Chen, K. Zhang et al.
- [Review—Recent Development of WO₃ for Toxic Gas Sensors Applications](#)
Doli Bonardo, Ni Luh Wulan Septiani, Fauzan Amri et al.
- [Gas sensing materials roadmap](#)
Huaping Wang, Jianmin Ma, Jun Zhang et al.

The sensitivity enhancement of TiO₂-based VOCs sensor decorated by gold at room temperature

Mostafa Shooshtari^{1,*} , Sten Vollebregt¹ , Yas Vaseghi², Mahshid Rajati³ and Saeideh Pahlavan⁴

¹Laboratory of Electronic Components, Technology, and Materials, Delft University of Technology, 2628 CD Delft, The Netherlands

²Department of Electrical Engineering, K.N. Toosi University of Technology, Tehran, Iran

³Department of Electrical and Computer Engineering, University of Windsor, Windsor, ON N9B 3P4, Canada

⁴School of Electrical and Computer Engineering, College of Engineering, University of Tehran, Tehran 14395-515, Iran

E-mail: mostafashooshtari@gmail.com and m.shooshari@tudelf.nl

Received 4 December 2022, revised 2 March 2023

Accepted for publication 23 March 2023

Published 6 April 2023



CrossMark

Abstract

Detection of hazardous toxic gases for air pollution monitoring and medical diagnosis has attracted the attention of researchers in order to realize sufficiently sensitive gas sensors. In this paper, we fabricated and characterized a Titanium dioxide (TiO₂)-based gas sensor enhanced using the gold nanoparticles. Thermal oxidation and sputter deposition methods were used to synthesize fabricated gas sensor. X-ray diffraction analysis was used to determine the anatase structure of TiO₂ samples. It was found that the presence of gold nanoparticles on the surface of TiO₂ enhances the sensitivity response of gas sensors by up to about 40%. The fabricated gas sensor showed a sensitivity of 1.1, 1.07 and 1.03 to 50 ppm of acetone, methanol and ethanol vapors at room temperature, respectively. Additionally, the gold nanoparticles reduce 50 s of response time (about 50% reduction) in the presence of 50 ppm ethanol vapor; and we demonstrated that the recovery time of the gold decorated TiO₂ sensor is less than 40 s. Moreover, we explain that the improved performance depends on the adsorption-desorption mechanism, and the chemical sensitization and electronic sensitization of gold nanoparticles.


Keywords: titanium dioxide, thermal oxidation, gas sensors, room temperature, volatile organic compounds

(Some figures may appear in colour only in the online journal)

1. Introduction

The ever-increasing use of automated vehicles in our era poses significant threats to human health and the environment.

* Authors to whom any correspondence should be addressed.

 Original content from this work may be used under the terms of the [Creative Commons Attribution 4.0 licence](https://creativecommons.org/licenses/by/4.0/). Any further distribution of this work must maintain attribution to the author(s) and the title of the work, journal citation and DOI.

Volatile organic compounds (VOCs) and hydrocarbons are examples of such threats. It has been demonstrated in many reports that the level of these pollutions can exceed the threshold limit value in residential areas. Monitoring and estimating these harmful toxic VOCs require highly precise, efficient, and reliable analytical devices. Metal oxide-based chemoresistive sensors are advantageous over other chemical sensors such as acoustic-based, optical and electro-analytical due to their ease of production, low cost and good portability [1]. Different metal oxides such as WO₃, SnO₂, ZnO, and TiO₂ have been reported as potentially promising candidates for gas

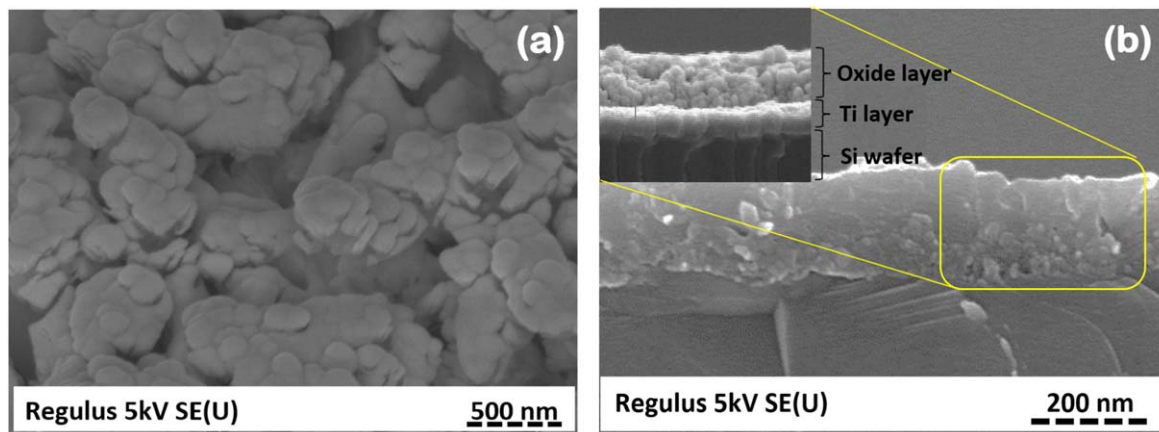


Figure 1. SEM images of the TiO_2 sample grown by thermal oxidation at 600°C for 4 h. (a) The surface of the oxide sample. (b) Cross-section image of the oxide.

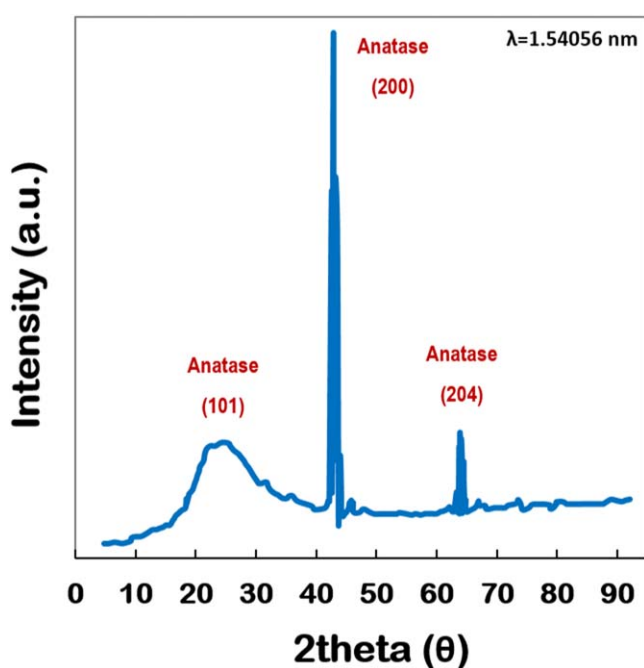


Figure 2. XRD analysis pattern of the titanium dioxide sample at 600°C .

sensing, whether applied individually or in composite structures [2]. TiO_2 , an n-type semiconductor material with high resistance and a bandgap of approximately 3 eV, has received great attention in the field of gas sensing as it is eco-friendly, chemically stable, and also has catalytic properties and allows for structural modulation [3]. The anatase phase of TiO_2 exhibits a high ability to react with gas molecules due to the large number of oxygen vacancies [4]. Thus, it is more commonly used in gas sensors than the Rutile and brookite phases. Various n-type TiO_2 structures -pristine or doped, composites- are employed to sense different types of VOCs such as ethanol, propanol, acetone, nitrogen oxide, carbon disulfide, and toluene [5].

Limitations of pristine TiO_2 sensors such as low sensitivity, high operating temperature, weak electrical stability, and non-selectivity are the most prominent remaining challenges. Thus, various methods have been proposed to overcome these

limitations. A reliable and effective method is the addition of noble metals such as gold, silver, platinum, and palladium, which can be performed during the synthesis of TiO_2 or after its completion [6, 7]. These noble metals change the electronic characteristics of TiO_2 , redesign the crystalline phases, and increase the density of surface defects. Thus, noble metals act as activators to improve gas response and selectivity and reduce the response and recovery time and operating temperature [8, 9]. In addition, noble metals have a greater impact on the gas sensing of TiO_2 nanostructures than other structures [5, 8].

One of the low-cost synthesis methods of Titanium dioxide nanoparticles in the form of thin-film is thermal oxidation. This growth method can lead to the formation of titanium dioxides in the anatase phase by controlling the air pressure in deposition systems [10]. The Titanium dioxide phase variance reported in the literature is generally attributed to the difference between the titanium layer nanostructure and its grain size [11, 12]. Oxidation starts from the surface and boundaries of the grains that the titanium film is composed of. The oxidation process continues until the titanium grain turns into titanium dioxide. The induced stress in the oxide changes its surface energy and controls the phase determination process. The oxidation temperature, pressure, and grain size affect the stress level. The higher the stress level gets, the higher the surface energy of the oxide becomes, and the oxide phase becomes anatase [13, 14]. Extensive research has been conducted regarding gold-decorated TiO_2 gas sensors [15–17]. However, a detailed review of existing studies demonstrates that nanoparticle-based gold-doped TiO_2 sensors still face challenges such as nanocomposites synthesis, operating temperature, response time, recovery time, and lifespan.

In this work, a VOC vapor sensor based on the decoration of TiO_2 nanoparticles was fabricated. The growth of TiO_2 nanoparticles was performed using the thermal oxidation method and the decoration of gold nanoparticles using a sputter deposition. Metal contacts were used to measure and analyze the electrical properties of the fabricated sensor. The structure, morphology, and topology of Au- TiO_2 layers were studied using the SEM, XRD, AFM, and EDX characterizations. The absorbance of the active layer was presented to evaluate the

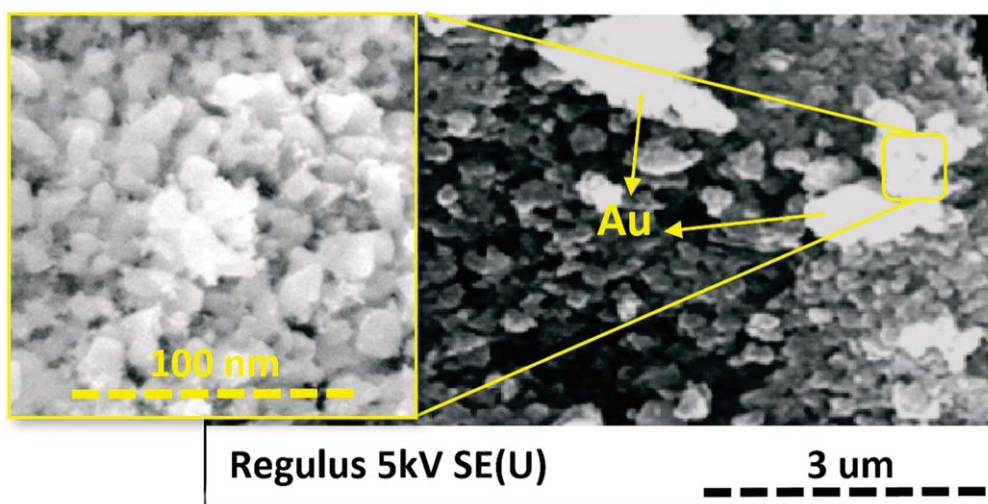


Figure 3. SEM images of the presence of gold nanoparticles on the surface of TiO₂.

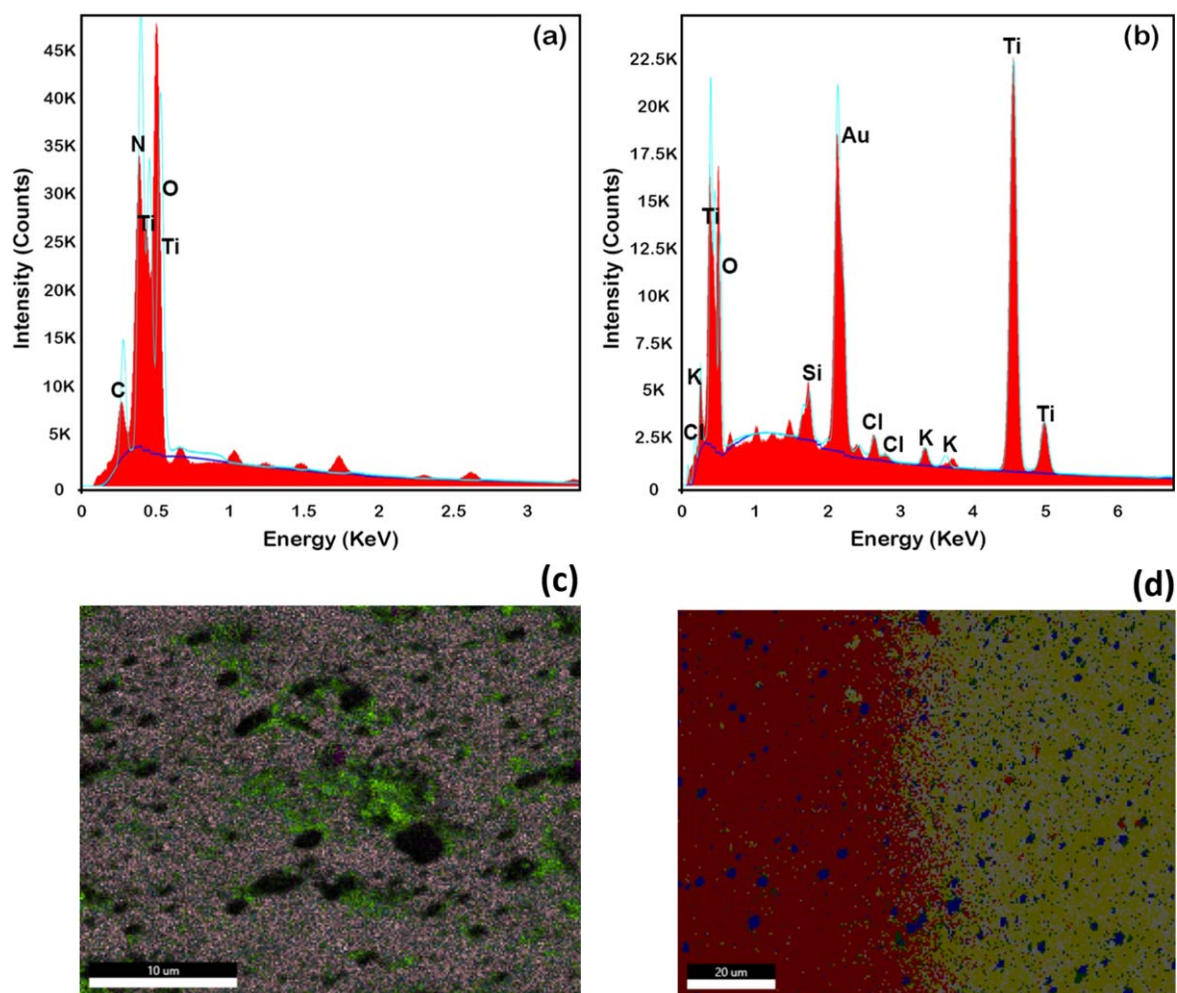


Figure 4. EDX spectrum of (a) TiO₂ (b) TiO₂ with gold nanoparticles and elemental mapping analysis of (c) TiO₂ (d) TiO₂ with gold nanoparticles.

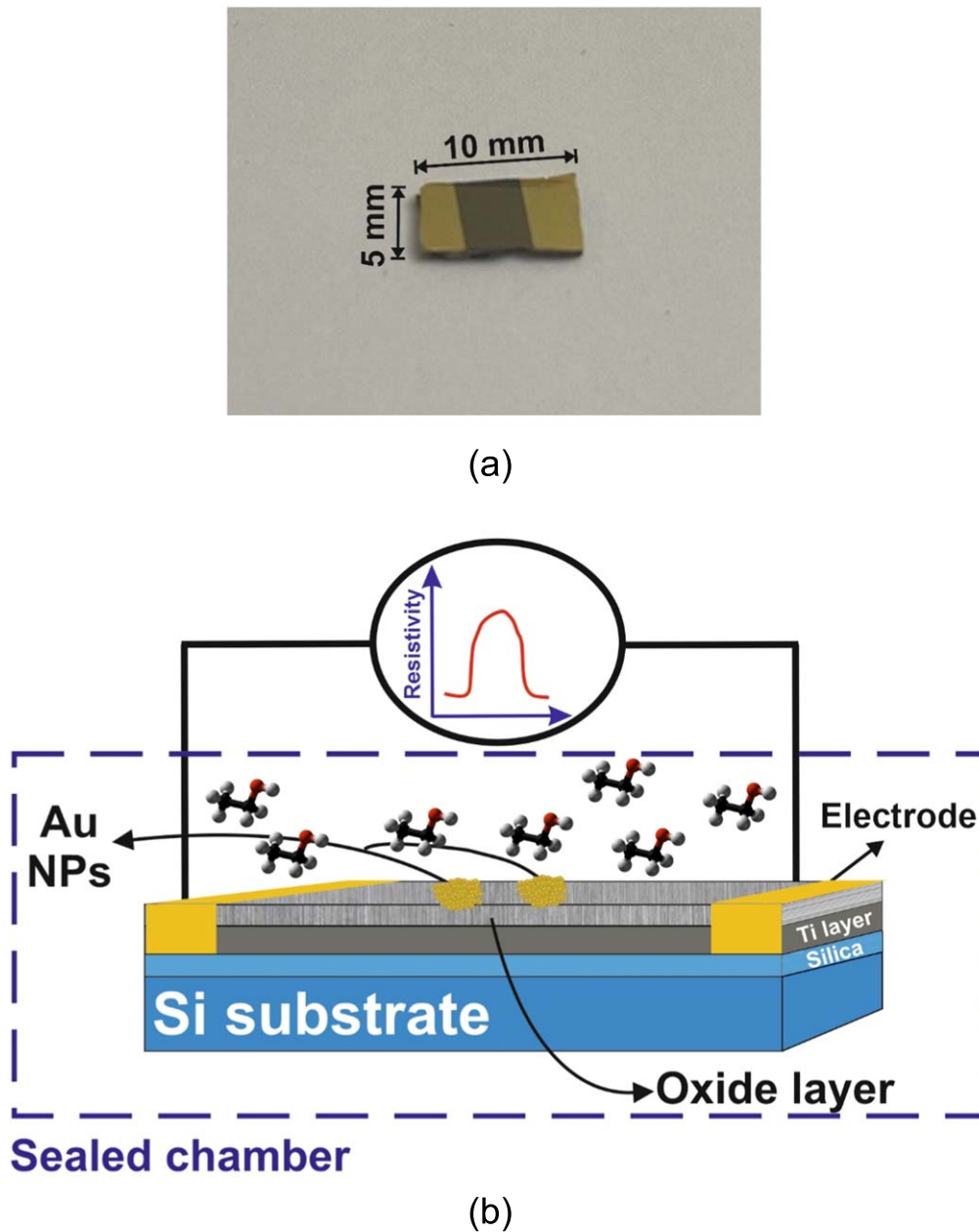


Figure 5. (a) The fabricated Au/TiO₂ sensor before connecting platinum wires. (b) Schematic diagram of the gas sensing measurement system.

bandwidth. Moreover, the gas sensor's sensitivity, selectivity, and transient response were studied.

2. Experimental section

2.1. Growth of titanium dioxide

A silicon wafer substrate with the dimensions of 5 mm × 10 mm was ultrasonically cleaned in acetone, ethanol, and distilled water consecutively for 5 min. A titanium thin film was deposited on the surface of Si/SiO₂ using an e-beam evaporator system. The Si/SiO₂ substrate was fixed on a rotating holder. The device was cleaned under vacuum

conditions for 15 min by argon ion beam and with 100 V DC voltage and 2 A current. A titanium layer of 100 nm was grown at a rate of approximately 0.05 nm per second. The growth temperature was kept at 100 °C before the deposition process and then at 150 °C during the growth process. During the growth process, the holder's spin speed was determined at 5 rpm so that a uniform growth is performed. Next, the sample was placed inside a furnace in the presence of air and at 600 °C for 4 h. This annealing process resulted in the growth of a titanium dioxide layer with a thickness of approximately 50 nm on a titanium layer with a thickness of about 70 nm. Obtained SEM top and cross-sectional images of TiO₂ are shown in figure 1. As shown in figure 1(a), the growth of the oxide on the surface of titanium has increased

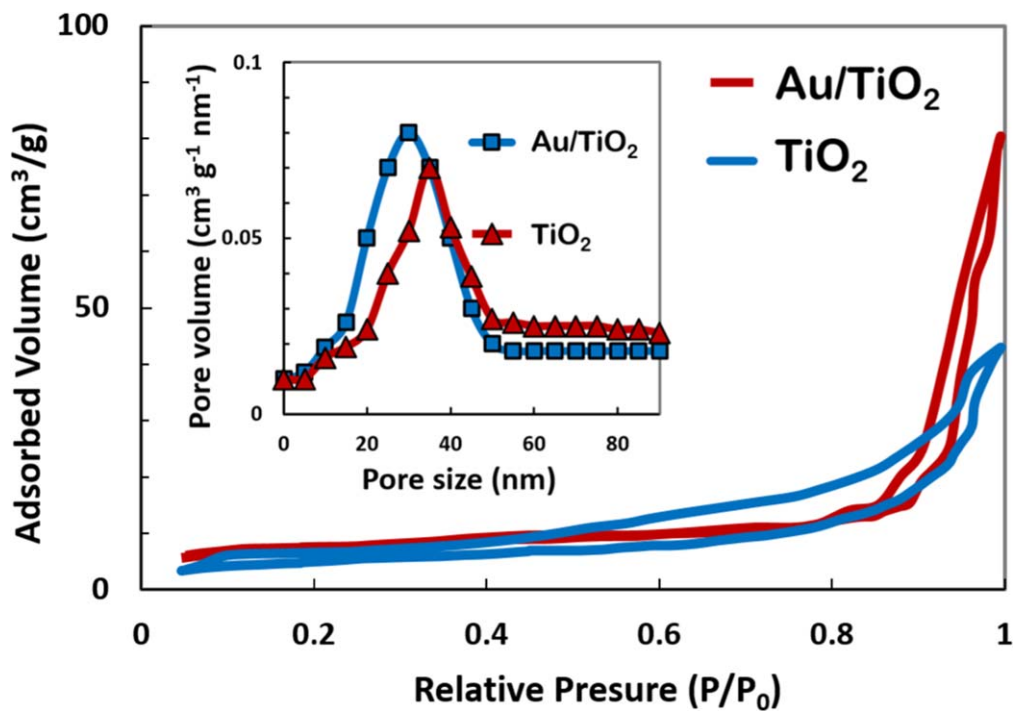


Figure 6. Nitrogen adsorption-desorption of TiO_2 and TiO_2/Au sensors.

Table 1. Surface area, pore-volume, and pore diameter of the TiO_2 and TiO_2/Au sensors.

Sample	S_{BET} ($\text{m}^2 \text{g}^{-1}$)	V_p ($\text{cm}^3 \text{g}^{-1}$)	D_p (nm)
TiO_2	16.78	0.11	33.2
Au/TiO_2	17.03	0.05	30.8

the thickness of the sample, which corresponds to the positive coefficient of titanium's thermal oxidation growth rate [18]. Figure 1(b) displays high porosity on the surface of the obtained oxide. The mentioned porosity and the existence of grain boundaries are important factors in gas sensing [12, 19, 20].

XRD analysis (Inel, EQUINOX3000, 40 kV and 25 mA) was employed to determine the crystalline phase of the obtained TiO_2 layers. In XRD equipment monochromatic optic $K\alpha_1$ or $K\alpha_{1/2}$ were used. It was found that the oxide grown on the titanium layer at 600 °C exhibits an anatase phase. Figure 2 shows the XRD pattern of this sample.

2.2. Growth of gold nanoparticles

Decoration of the fabricated TiO_2 sample with gold nanoparticles was accomplished using a sputtering device under certain conditions. For this purpose, a 99.99% purity 2-inch diameter gold target was used. The chamber's temperature was kept at room temperature, and the pressure was held at 1×10^{-5} mTorr. The voltage and current for the argon beam were set to 100 V and 3 A, respectively. The distribution and size of gold nanoparticles were controlled by the sputtering time which was set to 2, 4, 6, 8 or 10 s.

After the deposition process, the sample was annealed at 100 °C for 5 h. Figure 3 shows SEM images of the decorated TiO_2 samples. As shown in figure 3, gold metal nanoparticles have grown irregularly and randomly on the porous surface of TiO_2 .

Identification of the elements present in the sample is possible through energy dispersive x-ray (EDX) analysis. The fabricated TiO_2 sensor was characterized by EDX, before and after its decoration with gold, using an FEI Nova Nanosem equipped with EDAX Octane detector. As shown in figure 4, the EDX spectrum of the sample containing gold nanoparticles has an energy peak of approximately 2 eV, which demonstrates the presence of gold in the sample. From the EDX analysis, it is roughly estimated that the atomic ratio percentage of gold to TiO_2 is 10%. This recognition was made because of the registered energy, which is characteristic of gold nanoparticles. The Si signals originate from the substrate. The homogenous distribution of constituent element can be seen in elemental mapping presented in figures 4(c)–(d).

2.3. Fabrication of the gas sensor

Gas sensing equipment and gas sensing test methods have been explained in our previous studies [21, 22]. Two ~ 3 mm wide, 200 nm thick gold stripe electrodes and a tantalum adhesive layer were deposited on the TiO_2 sample. Silver paste was used to ensure the electrical connections of the platinum wires. A sample of the prepared sensor and the schematic diagram of the measurement system is shown in figures 5(a) and (b), respectively.

The gas response was obtained by measuring the resistance of the two electrodes using a Sanwa handheld digital

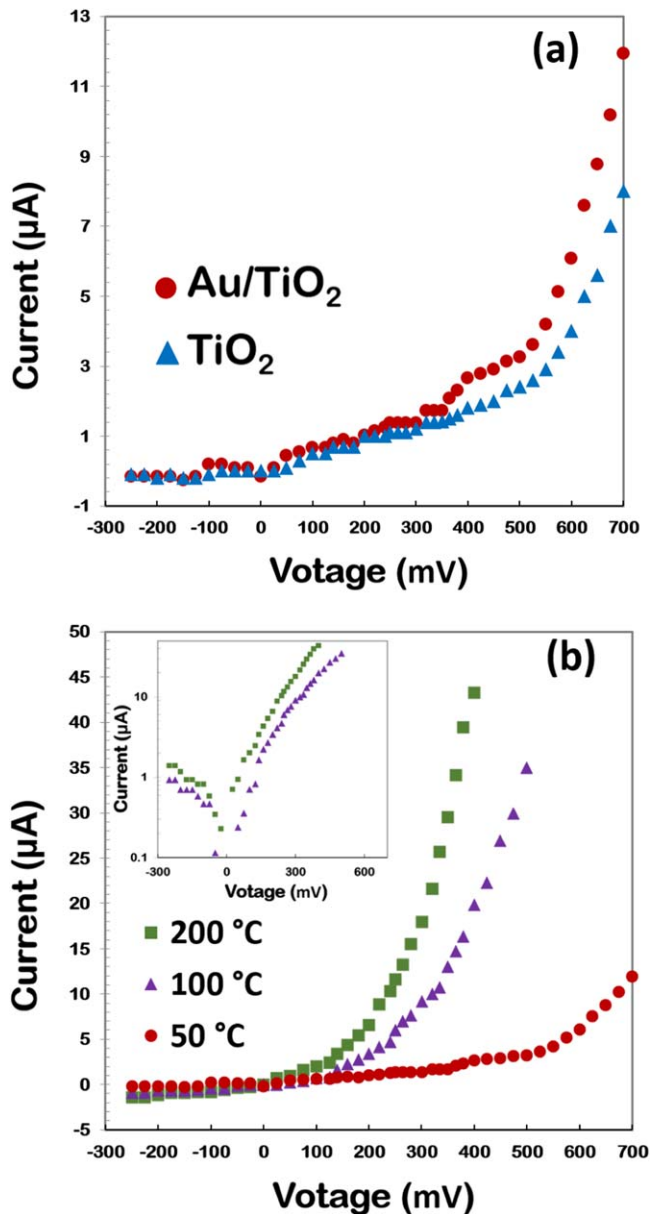


Figure 7. Typical current-voltage (I - V) characteristics of (a) TiO_2 -based sensor with and without Au nanoparticles and (b) in normal coordinates for Au/ TiO_2 contact at different temperatures. The inset curve in figure (b) presents a plot of I - V characteristics in semi-logarithmic scale.

CAT II multimeter. Room conditions were kept constant throughout all experiments ($25\text{ }^\circ\text{C}$ – $27\text{ }^\circ\text{C}$ temperature and 35%–45% Relative humidity).

The sensitivity of the gas sensor is expressed by the ratio of the measured resistance before exposure to gas to the measured resistance after it and is defined by the expression:

$$\text{SensitivityResponse} = \frac{R_a}{R_g} \quad (1)$$

where R_a and R_g are the sensor's resistance under room conditions (clean air) and in the presence of gas, respectively.

3. Results and discussion

3.1. Structural and morphological characteristics

N_2 adsorption-desorption isotherms were applied to the sensor. The surface area was investigated using a Brunauer-Emmet-Teller (BET) method.

Figure 6 displays N_2 adsorption-desorption isotherms and the pore size distribution diagram (BJH) of Au/ TiO_2 and pure TiO_2 samples. The sample shows an isotherm similar to type IV, which is representative of mesoporous solid [23]. Data regarding the pores' structure have been listed in table 1. Both samples demonstrate similar N_2 adsorption-desorption isotherms. Although surface areas with wide pore distribution can be seen in both samples, the gold-decorated sample has a larger pore volume and a smaller pore size compared to the TiO_2 sample. This difference in size and pore volume leads to an increase in the surface-to-volume ratio in the sensor. Increasing the volume-to-surface ratio course increases the sensitive surface to detect gas molecules. Therefore, gas response increases.

The output characteristics (I - V) of TiO_2 sensors before and after the decoration of gold on the TiO_2 are presented in figure 7(a). Both I - V curves show Schottky contact which indicates same contact before and after the decoration with gold nanoparticles. Due to the sparse nature of the gold nanoparticles, they had only a small impact on the conductivity of the sample [9, 24]. The I - V characteristic of the Au- TiO_2 sample at different temperatures has been demonstrated in figure 7(b) in order to investigate the electrical contact of the electrodes [25]. Since gold's work function ($W_{\text{Au}} = 5.1\text{ eV}$) [26] is larger than titanium dioxide's work function ($W_{\text{TiO}_2} = 4.6\text{ eV}$) [27], the contact between TiO_2 and Au causes the charge to transfer from the semiconductor (TiO_2) to gold (Au), and hence, a Schottky barrier forms at the junction. It has been demonstrated that the barrier height of the gold-titanium dioxide contact corresponds to the Schottky-Mott model, and the barrier's value varies between 0.9 and 1.2 eV [28, 29]. This difference is attributed to undesired surface states [30]. With due attention to the formed Schottky diode in the contact, all samples' resistance measurements were recorded at a voltage of 1 V to ensure reliable gas sensing results.

The optical response and optical bandgap of the layer are other criteria that help determine gold's dispersion in the TiO_2 thin film. Figure 8(a) shows the UV-vis absorption spectrum of TiO_2 and Au/ TiO_2 at room temperature. To removal substrate absorption effect in obtained UV-vis spectrum, original samples, samples on the glass substrate and Si substrate were measured separately. As can be observed in figure 8(a), TiO_2 exhibits a sharp absorption edge at about 400 nm, which is related to the bandgap excitation of TiO_2 [31]. Due to the uneven distribution of gold nanoparticles on the surface of Titanium dioxide, gold does not exhibit any evident absorption. Moreover, as SEM and EDX characterizations demonstrate, the actual Au content of Au/ TiO_2 is not

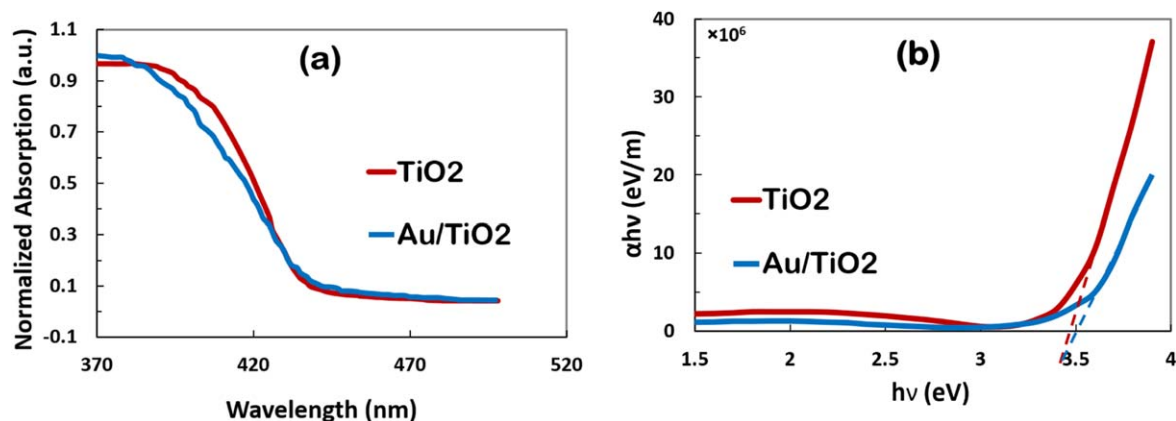


Figure 8. (a) Optical absorption spectrum of TiO₂ and Au/TiO₂ samples. (b) Optical band-energy spectra for TiO₂ and Au/TiO₂ thin films ($\alpha h\nu$ versus photon energy).

much, which might lead to the lack of a prominent absorption peak. Nevertheless, as can be seen in figure 8(a), a slight increase in light absorption is apparent in the Au/TiO₂ sample compared to the TiO₂ sample.

As shown in figure 8(a), the average adsorption in the range of 400–500 nm is below 10%. The bandgap of Au/TiO₂ can be determined using the adsorption of TiO₂ thin film in various wavelengths. Figure 8(b) shows the Tauc plot used to calculate the E_g of the Au/TiO₂ sample. This plot was used to obtain E_g and is based on equation (2):

$$(\alpha h\nu)^n = A(h\nu - E_g), \quad (2)$$

where α is the adsorption coefficient, A is the constant coefficient (band tailing parameter), $h\nu$ is the energy of the incident photon, and E_g is the bandgap energy. Extrapolation of the linear region obtains the bandgap on the $h\nu$ axis. The obtained E_g for the TiO₂ sample was calculated to be approximately 3.4 eV which corresponds to the literature [32]. Moreover, figure 8(b) demonstrates band gap energy obtain for the both samples. Based on the optical band-energy spectra shown in figure 8(b), it is clear that gold particles could change the light absorption behavior, as well as alter the optical bandgap of TiO₂. The optical bandgap is found to be composed and there is a slight increase in the bandgap of the TiO₂ with gold decoration. The doping of various transitional metal ions into TiO₂ could shift its optical absorption edge from the UV into the visible light range. Unlike TiO₂, which only absorbs light energy in the range of the UV spectrum, Au/TiO₂ absorbs additional light energy in the visible range due to the presence of the plasmonic phenomenon in the Au nanoparticles [33].

3.2. Gas sensing results

The fabricated sensors using bare TiO₂ and decorated TiO₂ were tested for sensing different VOC vapors. Figure 9 and the table inside it shows the sensing response of two gas sensor samples to 50 ppm of acetone, ethanol and ethanol vapors. As can be seen in figure 9, gold decoration does not lead to a significant change in sensitivity of the fabricated samples. As the gold-decorated TiO₂

has a sensitivity response of 1.13 to 50 ppm acetone vapor, while the intrinsic TiO₂ has a sensitivity of 1.1 in similar conditions. Gold decoration does significantly impacted the sensors' response time, such that the 100 s response time in the TiO₂ sensor decreased to about 50 s in the Au/TiO₂ sensor for 50 ppm of all tested VOC vapors. It should attribute to the catalytic promotion effect of Au, which leads to the decrease of activation energy and results in an increase of gas adsorption for the gas-sensing performance [34].

When the gas sensor is exposed to different concentrations of gas, the electrical conductivity of the active layer modulates the adsorption rate of gas molecules on the sensor surface. Gold nanoparticles in the form of discrete islands modify the surface structure of TiO₂. In an oxygen-rich atmosphere, oxidation of the nanometer islands provides a pair of Au⁺ and neutral Au in the equilibrium [35]. These redox pairs cause the formation of an electron depletion layer around the gold islands. The Schottky potential barrier formed at the Au⁰/Au⁺ pairs boundary causes carriers to increase [36]. This increase in effective carriers in gas sensing leads to the spillover effect. Therefore, the number of free electrons in the Au/TiO₂ sample is much larger than the number of free electrons in TiO₂. This fact is also confirmed by the current-voltage characteristic shown in figure 7(b). Because of the spillover effect, these trapped electrons cause the electron region to thicken and increase the oxygen adsorption sites [37]. Thus, the presence of gold nanoparticles on the surface of TiO₂ improves the Schottky barrier modulation in the oxidation process.

The sensing mechanism of the TiO₂ sensor is based on changes in the electrical conductivity of the sample at different atmospheric conditions. TiO₂, as an n-type semiconductor, adsorbs oxygen molecules to its surface when exposed to air, which results in the trapping of the electrons from the conduction band as shown in figure 10(a). The oxygen molecules are adsorbed in the forms of O_{2ads}⁻, O_{ads}⁻, or O_{ads}²⁻. Hence, the released h⁺ creates a space charge and causes a larger potential barrier to form [3, 38]. The increase in this potential leads to reduced electrical conductivity (see diagram on the left in figure 10(a)).

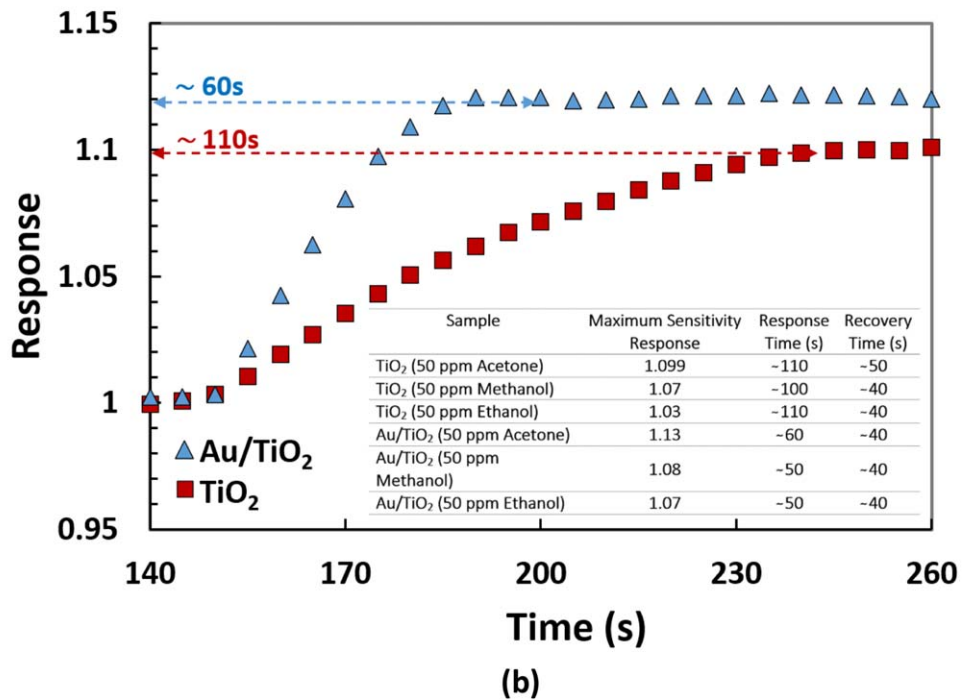
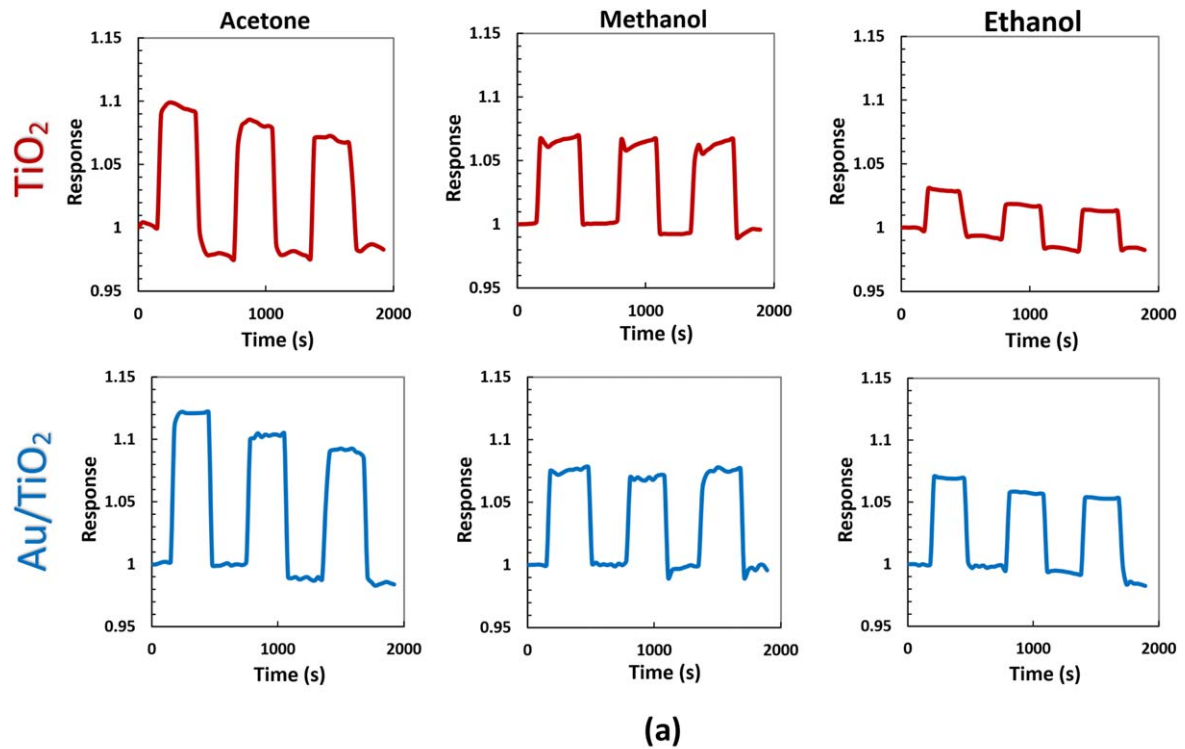
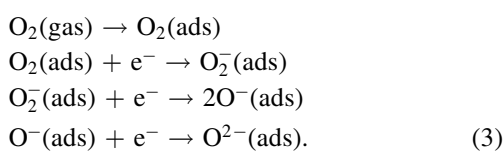


Figure 9. (a) Sensitivity response results of TiO₂ and Au/TiO₂ sensor toward 50 ppm methanol, ethanol, and acetone gas at room temperature. (b) Response area of Sensitivity curve of TiO₂ and Au/TiO₂ sensor toward 50 ppm acetone gas at room temperature (table inset is comparison of gas sensing parameters of TiO₂ and Au/TiO₂ samples).

This adsorption process can be defined according to equation (3):



When the sensor is exposed to gas molecules (see diagram on the right in figure 10(a)), its conductivity changes due to the reaction of the adsorbed oxygen species with gas molecules, and it releases back electrons to the conduction band. This process results in a smaller potential barrier and,

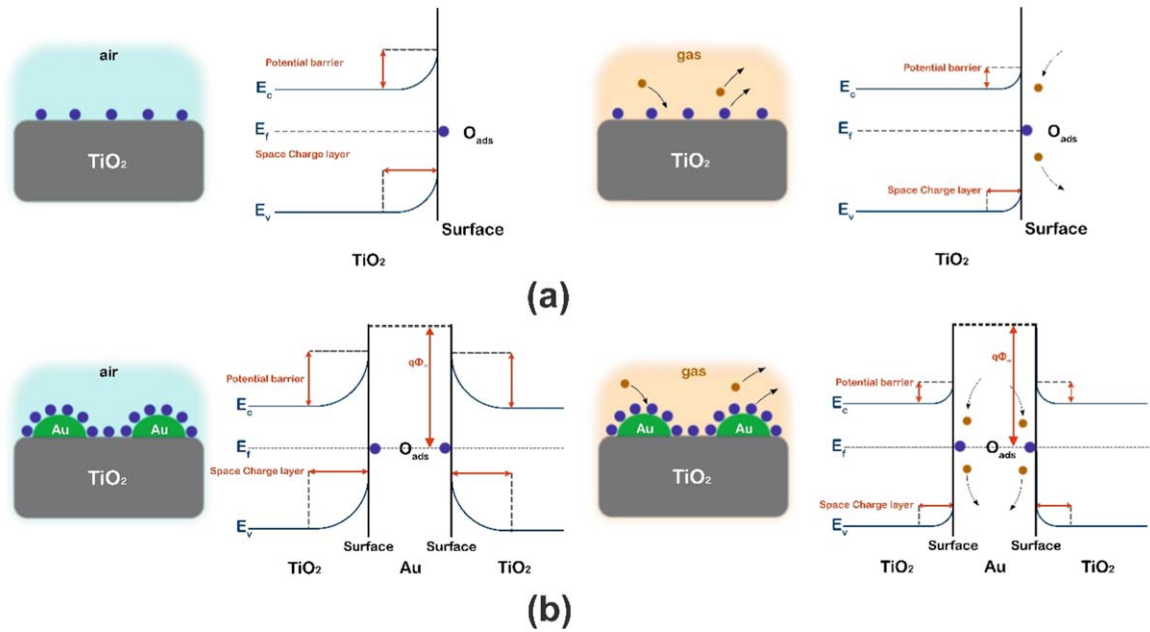


Figure 10. A schematic diagram of the reaction mechanism of the (a) TiO₂ and (b) Au/TiO₂ based gas sensor clean air and the presence of gas.

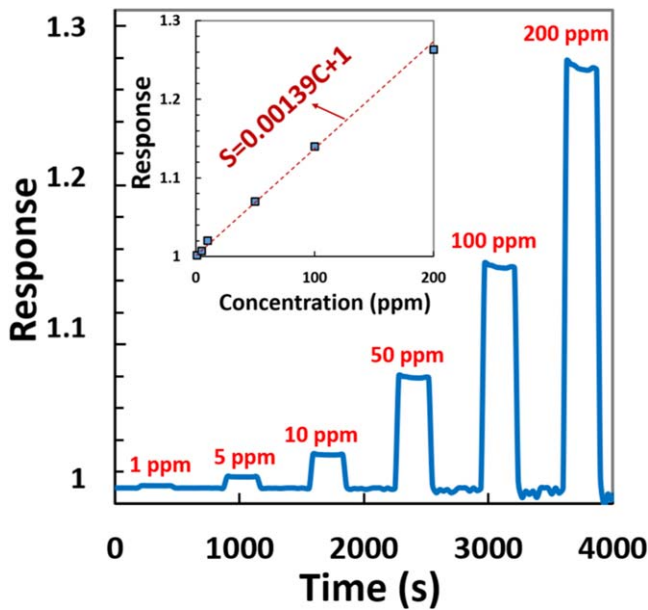
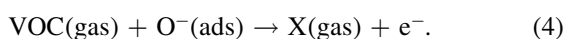


Figure 11. Typical dynamic response curves of Au/TiO₂ sensor for 1–200 ppm ethanol vapor at room temperature. The inset plot is the corresponding linear relationship of the sensitivity to concentration.

thus, increased conductivity. This process can be defined according to equation (4):



As figure 10(b) demonstrates, the increase in gas response can be described by electronic sensitization and chemical sensitization of Au catalyst. The different work functions of Au and TiO₂ on the gas adsorbent surface can lead to electron interaction between Au and TiO₂ and the

formation of an extra electron depletion layer on the joint surface. Therefore, when the surface oxygen molecules react with gas molecules, more carriers are released, which results in further change in electrical conductivity.

Figure 11 demonstrates the dynamic performance of Au/TiO₂ towards different concentrations (1–200 ppm) of ethanol gas at room temperature. Moreover, this figure shows the transient sensing curves and stable sensing and recovery of the TiO₂ sample. As can be seen in figure 11, increasing ethanol concentration causes more molecules to react with the adsorbed oxygen molecules, which leads to an increase in the sensor sensitivity. The sensitivity of the sensor to 1 ppm, 5 ppm, 10 ppm, 50 ppm, 100 ppm and 200 ppm ethanol gas was found to be 1.0014, 1.0069, 1.02, 1.07, 1.138 and 1.263, respectively. The fabricated sensor shows an acceptable response to low concentrations of ethanol vapor at room temperature, hence making it an appropriate option for low-power applications.

The dependency of the response as a function of ethanol concentration for the Au/TiO₂ sample is shown in the inset of figure 11. As can be seen in the figure, linearly increasing the concentration from 1 to 200 ppm significantly increases the response sensitivity. This linear dependency can be modeled by equation (5):

$$S \left(= \frac{R_a}{R_g} \right) = 0.00139C + 1 \quad (5)$$

where S is the sensitivity and C is ethanol vapor concentration. Moreover, the detection limit of the sensor of 0.22 ppm was recorded. The limit of detection was obtained theoretically by using extrapolation of the sensitivity curve till it hits the noise level of the device [39].

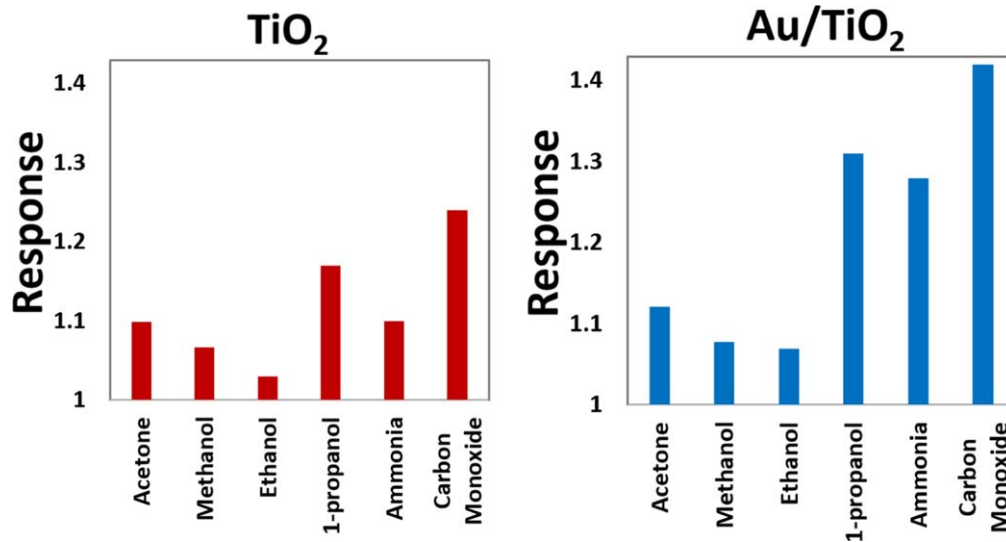


Figure 12. Comparison of the sensitivity response of the fabricated sensors in the presence of 50 ppm of 6 different gases.

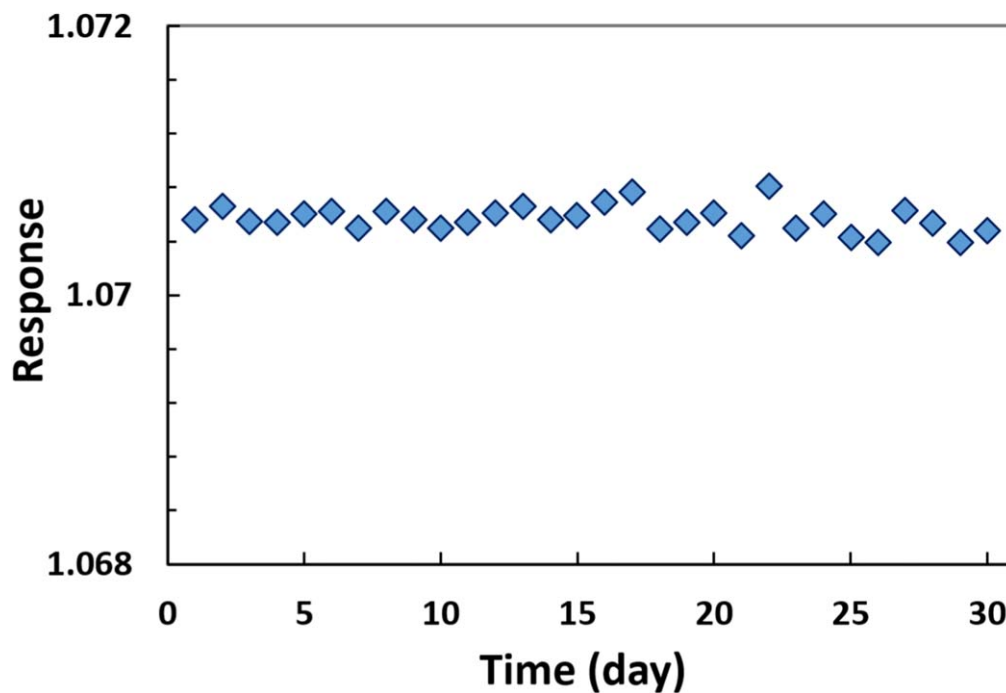


Figure 13. Long-term stability of Au/TiO₂ sensor towards 50 ppm ethanol vapor at room temperature.

Another important factor when studying sensor performance is selectivity, which is the ability of sensors to show a precise response to the target gas in the presence of different gases [22, 40]. Both TiO₂ and Au-TiO₂ sensor structures were exposed to 50 ppm six different gases, including acetone, ethanol, methanol, 1-propanol, ammonia, and carbon monoxide. Figure 12 shows the sensitivity of the fabricated sensors in the presence of different gases. The decorated sample did not exhibit increased selectivity for any of the studied gases.

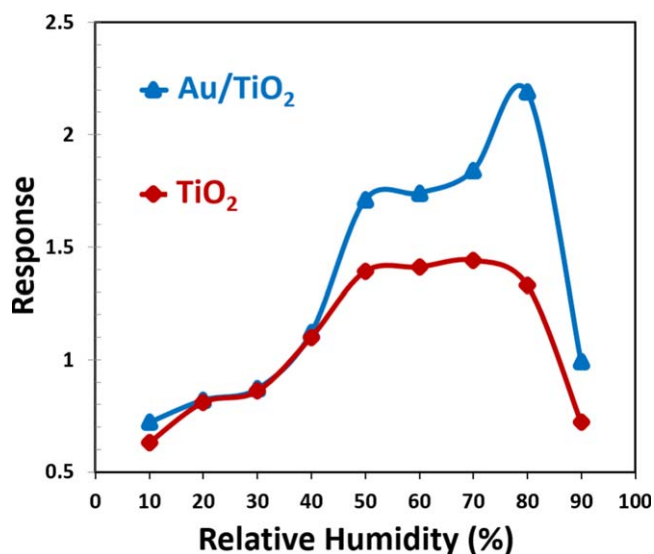
Long-term stability is another one of the gas sensor's important factors, and it demonstrates the reliability of the sensor [41]. The stability of the decorated TiO₂ sensor in the

presence of 50 ppm ethanol was evaluated at room temperature. As is evident in figure 13, the relative deviation of the gas response sensitivity was less than 2% in the first 15 d and about 3% in the following 15 d.

Moreover, the effect of humidity on the sensing mechanism of the fabricated sensors was investigated. Figure 14 shows the response sensitivity as a function of the applied relative humidity to TiO₂ and Au/TiO₂ sensors when exposed to 50 ppm acetone vapor. It is found that the effect of humidity on tested TiO₂ and Au/TiO₂ gas sensors is similar to the impact of humidity on the nanowire TiO₂ ethanol vapor sensors [3]. To ensure the responses obtained from the gas testing results, two other samples with the same experimental

Table 2. Comparison of acetone sensing parameters of TiO₂- based sensor of this work and those reported in the literature.

Materials	Method	Sensitivity	Response time (s)	Recovery time (s)	Concentration (ppm)	Operating temperature (°C)
Au/TiO ₂ (This study)	Thermal oxidation	~1.13	~60	40	50	Room temperature
TiO ₂ Nano-particles [42]	Hydrothermal	9	10	9	500	270
TiO ₂ nanobelt [43]	Hydrothermal	~10	~12	16	500	(240–340)
Nanorod TiO ₂ [44]	Hydrothermal	~5	6	500	200	400
Nanotube TiO ₂ [45]	Electrochemical anodization	2.5	17	26	1000	150

**Figure 14.** The variation of the sensitivity response of TiO₂ and Au/TiO₂ sensors as a function of relative humidity during the exposure to 50 ppm acetone at room temperature.

conditions were fabricated for each type of sensor. Recorded gas sensitivity parameters of other samples guarantee all results.

Table 2 demonstrates a comparison of the current research with similar studies in key sensing parameters such as sensitivity, gas concentration, response and recovery time. As can be observed, different TiO₂ structures (such as TiO₂ nanobelt, Au-TiO₂ nanoparticles, etc) were employed to detect different VOC gases, especially ethanol. Among them, we employed a simple growth method to obtain porosity and Au decoration at room temperature, which demonstrated satisfactory results compared to other works.

4. Conclusion

A TiO₂ gas sensor was fabricated through thermal oxidation with process control to increase porosity. Gold nanoparticles were deposited on the surface of the fabricated sensor by the sputtering technique. The developed sensors are capable to detect low concentrations of VOC vapors at room temperature. Close observation indicates that gold decoration leads to an increased sensitivity towards VOC vapors. Pure TiO₂

and Au/TiO₂ exhibited a sensitivity percentage of 3% and 7% towards 50 ppm ethanol vapor, respectively. Moreover, it was found that the response time of the decorated sample had improved by 50% compared to pure TiO₂. The sensors showed no degradation in their response over a period of 30 d. Thus, this research can provide the basis for further extensive studies on enhancing the gas sensor's performance of VOC sensors. To continue this research using other noble metals as catalysts are recommended.

Data availability statement

All data that support the findings of this study are included within the article (and any supplementary files).

ORCID iDs

Mostafa Shooshtari  <https://orcid.org/0000-0003-1292-0683>

Sten Vollebregt  <https://orcid.org/0000-0001-6012-6180>

References

- [1] Lin T *et al* 2019 Semiconductor metal oxides as chemoresistive sensors for detecting volatile organic compounds *Sensors* **19** 233
- [2] Dey A 2018 Semiconductor metal oxide gas sensors: a review *Mater. Sci. Eng.B* **229** 206–17
- [3] Shooshtari M, Salehi A and Vollebregt S 2021 Effect of temperature and humidity on the sensing performance of TiO₂ nanowire-based ethanol vapor sensors *Nanotechnology* **32** 325501
- [4] Chen X, Hosseini S N and van Huis M A 2022 Heating-induced transformation of anatase TiO₂ nanorods into rock-salt TiO nanoparticles: implications for photocatalytic and gas-sensing applications *ACS Appl. Nano Mater.* **5** 1600–6
- [5] Tian X *et al* 2021 Gas sensors based on TiO₂ nanostructured materials for the detection of hazardous gases: a review. *nano Mater. Sci.* **3** 390–403
- [6] Simonetti E A N *et al* 2021 TiO₂ as a gas sensor: the novel carbon structures and noble metals as new elements for enhancing sensitivity—a review *Ceram. Int.* **47** 17844–76
- [7] Zhu H *et al* 2021 Improved acetone sensing characteristics of TiO₂ nanobelts with Ag modification *J. Alloys Compd.* **887** 161312

- [8] Liu C *et al* 2015 The effect of noble metal (Au, Pd and Pt) nanoparticles on the gas sensing performance of SnO₂-based sensors: A case study on the {221} high-index faceted SnO₂ octahedra *CrystEngComm*. **17** 6308–13
- [9] Shooshtari M *et al* 2022 Enhancement of room temperature Ethanol sensing by optimizing the density of vertically aligned carbon nanofibers decorated with gold nanoparticles *Materials* **15** 1383
- [10] Diamanti M V *et al* 2009 Effect of thermal oxidation on titanium oxides' characteristics *J. Exp. Nanosci.* **4** 365–72
- [11] Zhu K-R *et al* 2005 Size effect on phase transition sequence of TiO₂ nanocrystal *Mater. Sci. Eng.A* **403** 87–93
- [12] Shooshtari M and Salehi A 2021 Ammonia room-temperature gas sensor using different TiO₂ nanostructures *J. Mater. Sci., Mater. Electron.* **32** 17371–81
- [13] Vaquila I *et al* 1999 Chemical reactions at surfaces: titanium oxidation *Surf. Coat. Technol.* **122** 67–71
- [14] Wang G *et al* 2016 Surface thermal oxidation on titanium implants to enhance osteogenic activity and in vivo osseointegration *Sci. Rep.* **6** 1–13
- [15] Hu L *et al* 2016 Au nanoparticles decorated TiO₂ nanotube arrays as a recyclable sensor for photoenhanced electrochemical detection of bisphenol *Environ. Sci. Technol.* **50** 4430–8
- [16] Mintcheva N *et al* 2020 Room-temperature gas sensing of laser-modified anatase TiO₂ decorated with Au nanoparticles *Appl. Surf. Sci.* **507** 145169
- [17] Zhang S *et al* 2022 Enhanced sensing performance of Au-decorated TiO₂ nanospheres with hollow structure for formaldehyde detection at room temperature *Sensors Actuators B* **358** 131465
- [18] Zhou B *et al* 2013 Preparation and characterization of TiO₂ thin film by thermal oxidation of sputtered Ti film *Mater. Sci. Semicond. Process.* **16** 513–9
- [19] Wang L *et al* 2019 Grain-boundary-induced drastic sensing performance enhancement of polycrystalline-microwire printed gas sensors *Adv. Mater.* **31** 1804583
- [20] Ra H *et al* 2010 The effect of grain boundaries inside the individual ZnO nanowires in gas sensing *Nanotechnology* **21** 085502
- [21] Shooshtari M, Salehi A and Vollebregt S 2020 Effect of humidity on gas sensing performance of carbon nanotube gas sensors operated at room temperature *IEEE Sens. J.* **21** 5763–70
- [22] Shooshtari M and Salehi A 2022 An electronic nose based on carbon nanotube-titanium dioxide hybrid nanostructures for detection and discrimination of volatile organic compounds *Sensors Actuators B* **357** 131418
- [23] Yang P *et al* 1998 Generalized syntheses of large-pore mesoporous metal oxides with semicrystalline frameworks *Nature* **396** 152–5
- [24] Huang C *et al* 2021 One-step fabrication of highly dense gold nanoparticles on polyamide for surface-enhanced Raman scattering *Appl. Surf. Sci.* **561** 149856
- [25] Shooshtari M *et al* 2022 Investigating organic vapor sensing properties of composite carbon nanotube-zinc oxide nanowire *Chemosensors* **10** 205
- [26] Lang N and Kohn W 1971 Theory of metal surfaces: work function *Phys. Rev.B* **3** 1215
- [27] Kashiwaya S *et al* 2018 The work function of TiO₂ *Surfaces* **1** 73–89
- [28] McFarland E W and Tang J 2011 *A Photovoltaic Device Structure Based On Internal Electron Emission, In Materials For Sustainable Energy: A Collection of Peer-Reviewed Research and Review Articles from Nature Publishing Group.* ed D Vincent (Singapore: World Scientific) pp 85–7
- [29] Tang J *et al* 2003 Electrochemical fabrication of large-area Au/TiO₂ junctions *Electrochem. Commun.* **5** 497–501
- [30] Jerisian R, Loup J and Gautron J 1984 Influence of oxygen on the behaviour of diodes fabricated from sputtered TiO₂ films on gold *Thin Solid Films* **115** 229–35
- [31] Duan Z *et al* 2019 Electrospinning fabricating Au/TiO₂ network-like nanofibers as visible light activated photocatalyst *Sci. Rep.* **9** 1–8
- [32] Karkare M M 2014 Estimation of band gap and particle size of TiO₂ nanoparticle synthesized using sol gel technique 2014 *Int. Conf. on Advances in Communication and Computing Technologies (ICACACT 2014)* (IEEE)
- [33] Wu J C and Chen C H 2004 A visible-light response vanadium-doped titania nanocatalyst by sol-gel method *J. Photochem. Photobiol. A* **163** 509–15
- [34] Peng S *et al* 2019 Pt decorated SnO₂ nanoparticles for high response CO gas sensor under the low operating temperature *J. Mater. Sci., Mater. Electron.* **30** 3921–32
- [35] Navaneethan M *et al* 2018 Sensitivity enhancement of ammonia gas sensor based on Ag/ZnO flower and nanoellipsoids at low temperature *Sensors Actuators B* **255** 672–83
- [36] Liang J *et al* 2018 Room temperature NO₂ sensing properties of Au-decorated vanadium oxide nanowires sensor *Ceram. Int.* **44** 2261–8
- [37] Cai J *et al* 2021 Surface oxygen vacancies promoted Pt redispersion to single-atoms for enhanced photocatalytic hydrogen evolution *J. Mater. Chem.A* **9** 13890–7
- [38] Li Z *et al* 2018 Resistive-type hydrogen gas sensor based on TiO₂: A review *Int. J. Hydrogen Energy* **43** 21114–32
- [39] Suematsu K, Harano W, Oyama T, Shin Y, Watanabe K and Shimanoe K 2018 Pulse-driven semiconductor gas sensors toward ppt level toluene detection *Anal. Chem.* **90** 11219–23
- [40] Wusiman M and Taghipour F 2022 Methods and mechanisms of gas sensor selectivity *Crit. Rev. Solid State Mater. Sci.* **47** 416–35
- [41] Chen W *et al* 2012 Gas sensing properties and mechanism of nano-SnO₂-based sensor for hydrogen and carbon monoxide *J. Nanomater.* **2012** 1
- [42] Navale S *et al* 2018 Enhanced acetone sensing properties of titanium dioxide nanoparticles with a sub-ppm detection limit *Sensors Actuators B* **255** 1701–10
- [43] Chen N *et al* 2017 Acetone sensing performances based on nanoporous TiO₂ synthesized by a facile hydrothermal method *Sensors Actuators B* **238** 491–500
- [44] Sun G-J *et al* 2016 Synthesis of TiO₂ nanorods decorated with NiO nanoparticles and their acetone sensing properties *Ceram. Int.* **42** 1063–9
- [45] Bhattacharyya P, Bhowmik B and Fecht H-J 2015 Operating temperature, repeatability, and selectivity of TiO₂ nanotube-based acetone sensor: influence of Pd and Ni nanoparticle modifications *IEEE Trans. Device Mater. Reliab.* **15** 376–83